

Effects of changes in use and soil cover on real evapotranspiration from the creation of a remote sensing product in the Xingu basin

Efeitos das mudanças de uso e cobertura do solo na evapotranspiração real com base na criação de um produto de sensoriamento remoto na bacia do Xingu

Sarah Christina Ribeiro Antunes¹ , Celso Bandeira de Melo Ribeiro¹ , Ricardo Neves de Souza Lima² , Augusto Getirana³ 

ABSTRACT

Several studies have shown that changes in land cover within a given watershed significantly affect the hydrological cycle and its variables. In the Xingu basin, many areas had their vegetation replaced by agricultural crops and pastures, while deforestation has been particularly prevalent in the region known as the Arch of Deforestation. Using remote sensing techniques enable the estimation of biophysical variable ETr for extensive areas, as exemplified in the study basin. Evapotranspiration data used in this work were obtained by creating a product that returns the combined median of the MOD16A2, PML_V2, Terra Climate, GLEAM_v3.3a, FLUXCOM, SSEBop, FLDAS, and ERA5-Land models, with subsequent application of the data provided by Collection 6 of the MapBiomas network, allowing the integration of land use and land cover information with real evapotranspiration estimates for the transition ranges: Forest to Pasture; Forest to Agricultural Land; Cerrado to Pasture; Cerrado to Agricultural Land. The interval defined for the study corresponds to the years 1985 to 2020, according to the historical series available on MapBiomas. After applying programming languages to filter the data, the results underwent statistical analysis to elucidate the effects of soil changes on evapotranspiration. Over the total data period (1985–2020), there was a decrease in forest areas (-16.23%), with conversion to pasture areas, in the order of +12.51%, and agricultural areas, reaching +5.5%. In the same timeframe, evapotranspiration in conversion bands underwent minimal changes, notably from 2009 to 2020, where a decreasing trend was reported of 0.095 mm/month for the “forest to pasture” substitution, and 0.090 mm/month in “Cerrado for pasture”.

Keywords: MapBiomas; Cerrado; Amazon.

RESUMO

Diversos estudos comprovaram que as mudanças na cobertura da terra de bacias hidrográficas afetam o ciclo hidrológico e suas variáveis. Na bacia do Xingu muitas áreas tiveram a substituição da vegetação por cultivos agrícolas e pastagens, enquanto outras foram desmatadas, principalmente na região do Arco do Desmatamento. Com as técnicas de sensoriamento remoto, é possível estimar a variável biofísica ETr para grandes áreas, que configura o caso da bacia de estudo. Os dados de evapotranspiração utilizados neste trabalho foram obtidos por meio da criação do produto que retorna a mediana conjugada dos modelos MOD16A2, PML_V2, Terra Climate, GLEAM_v3.3a, FLUXCOM, SSEBop, FLDAS e ERA5-Land, com posterior aplicação dos dados fornecidos pela Coleção 6 da rede MapBiomas, permitindo a união do uso e cobertura do solo com a estimativa da evapotranspiração real para as faixas de conversão: floresta para pasto; floresta para terra agrícola; cerrado para pasto; cerrado para terra agrícola. O intervalo definido para o estudo corresponde aos anos de 1985 a 2020, conforme a série histórica disponível no MapBiomas. Após a aplicação de linguagens de programação para filtrar os dados provenientes, os resultados foram submetidos a testes estatísticos capazes de relacionar os efeitos causados pelas alterações do solo na evapotranspiração. No período total de dados (1985–2020), foram constatados decréscimos nas áreas de floresta (-16,23%), com conversão em áreas de pastagens na ordem de +12,51% e em áreas agrícolas chegando a +5,5%. No mesmo período, a evapotranspiração nas faixas de conversão sofreu alterações ínfimas, tendo destaque apenas no intervalo 2009–2020, quando foi reportada tendência de decréscimo de 0,095 mm/mês para a substituição “floresta para pasto” e a 0,090 mm/mês em “cerrado para pasto”.

Palavras-chave: MapBiomas; Cerrado; Amazônia.

¹Universidade Federal de Juiz de Fora – Juiz de Fora (MG), Brazil.

²Instituto Brasileiro de Geografia e Estatística – Rio de Janeiro (RJ), Brazil.

³NASA Goddard Space Flight Center – Greenbelt (MD), United States.

Correspondence author: Sarah Christina Ribeiro Antunes – Rua Eduardo Sathler, 605 – Serra D’Água – CEP: 36035-720 – Juiz de Fora-(MG), Brazil. E-mail: sarah.ribeiro@engenharia.ufjf.br

Conflicts of interest: the authors declare no conflicts of interest.

Funding: none.

Received on: 06/24/2023. Accepted on: 01/18/2024.

<https://doi.org/10.5327/Z2176-94781658>



This is an open access article distributed under the terms of the Creative Commons license.

Introduction

To ensure the efficient management of water resources, it is essential to access reliable databases about the hydrological variables that characterize a given basin. For instance, understanding the actual evapotranspiration (ET) associated with each type of cover and land use, which helps in sustainable natural resource management (Saddique et al., 2020; Cabral Júnior et al., 2022).

It is well-established that changes in land use and land cover have an impact on climate (Alves et al., 2021; Rossatto et al., 2022), biological diversity (Sala et al., 2000; Galina et al., 2022), as well as on hydrological and biogeochemical cycles (Marinho Junior et al., 2020). Numerous studies have shown that deforestation significantly reduces precipitation and ET (Costa and Foley, 2000; Nóbrega, 2014; Santos et al., 2017; Saddique et al., 2020). Other works carried out in the Amazon Forest highlight the impact of vegetation cover changes on the water balance (Pongratz et al., 2006; Hayhoe et al., 2011; Griffiths et al., 2018; Cabral Júnior et al., 2022) and actual ET (Souza et al., 2019; Kohler et al., 2021; Paiva et al., 2023).

According to the Brasil Revealed Report produced by MapBiomas (2022), out of the 44.5 million hectares deforested on a large scale, primarily along the margins of the remaining Amazon Forest, about 13.6% were converted to agricultural land and 86.3% into pastures. In this context, it is clear that deforestation causes a decrease in ET rates, especially during the dry season (Caioni, 2021; Zhang et al., 2022; Paiva et al., 2023).

Vegetation plays a crucial role in calculating the energy balance and in the water flow, as it directly stores a portion of the precipitated volume through its foliage, allowing the transpiration of this water into the environment, contingent upon the potential evaporation capacity (Hewlett and Hibbert, 1967; Pritchett, 1979). In this context, the presence of vegetation in the soil promotes water infiltration, varying according to land use and occupation characteristics. This underscores the fundamental relationship between soil-vegetation-atmosphere, which directly influences basin ET (Hewlett and Hibbert, 1967).

The Xingu Hydrographic Basin is characterized by the convergence of the Cerrado and Amazon biomes, located in the southern and northern portions of the territory, respectively, with transitional formations in the central portions. Each of the forming ecosystems provides different climatic, ecological, vegetation and soil use particularities. Due to such plurality, the Xingu basin became a focal point for the exploitation of land and natural resources, expanding agricultural frontiers, pastures, and cattle ranching to the detriment of native vegetation cover (Isa, 2012; Lucas et al., 2021).

Furthermore, the Xingu basin stands out as the most threatened area in the entire Brazilian portion of the Amazon, holding alarming deforestation records, mainly in Environmental Protection Areas (EPA) such as Triunfo do Xingu and the Cachoeira Seca indigenous lands, Ituna Itatá, and Apyterewa (Rede Xingu+, 2021). In short,

changes in land use and management result not only from deforestation but also from selective raw materials extraction, burning practices, urbanization characteristics and, the replacement of vegetation by impermeable surfaces and/or cultivation of new crops, for example.

The analysis of land use and land cover, based on geoprocessing and remote sensing techniques, emerges as an essential tool for spatial analysis, since it facilitates the swift evaluation of geographic scenarios and enables more assertive decision-making in the area (Paranhos Filho et al., 2014; Rothmund et al., 2019; Vendruscolo et al., 2022). Both actual ET and land use and cover data are pivotal for effective river basin management. Given the challenges in obtaining such data, remote sensing tools stand out from the rest, allowing the estimation of parameters regardless of the dimensions of the area of interest (Rodrigues et al., 2019). Through this technique, spatially distributed hydrological variables can be directly acquire (Warren, 2013; Oliveira et al., 2020).

Given this context, the noticeable scarcity of studies focused on the Xingu, particularly those analyzing the impact of land use and land cover on real ET, is evident. The need for updates and potentially effective studies in such an area, divided between the Amazon and the Cerrado, is also characterized as a significant factor. For this reason, the present work used the region comprised by the Xingu basin, which is large and formed by the union of these biomes, as a study area in order to investigate possible correlations between the types of land use and land cover and ET. This is achieved through the application of remote sensing techniques, aiming to scrutinize the spatial dynamics of real evapotranspiration (ETr).

Methodology

Studying area

The study area is located within the Xingu basin, comprising the division of the states of Mato Grosso and Pará, Brazil, and encompassing the ecological conversion of the Cerrado and Amazon biomes, covering approximately 531,250 km² (Figure 1). Due to its natural constitution, the precipitation levels in the basin range from 1,500 to 2,500 mm/year, directly influencing ET values. Such data are influenced by the climate variability of the region, positioned between the Equatorial climate to the north, and the Tropical, to the south (Lucas et al., 2009; Isa, 2016; Rizzo et al., 2020; Cunha et al., 2023).

Given the latitudinal extension of the Xingu basin, the classification of its soils is represented here according to the biomes that form the area. In both the Amazon and Cerrado regions, the predominance of latosols is observed, with specific differences. While Amazonian oxisols boast considerable depth and good drainage, Cerrado oxisols have a higher percentage of organic matter and are visibly even more weathered. Parallel to soil classification, vegetation cover also exerts an influence on ET.

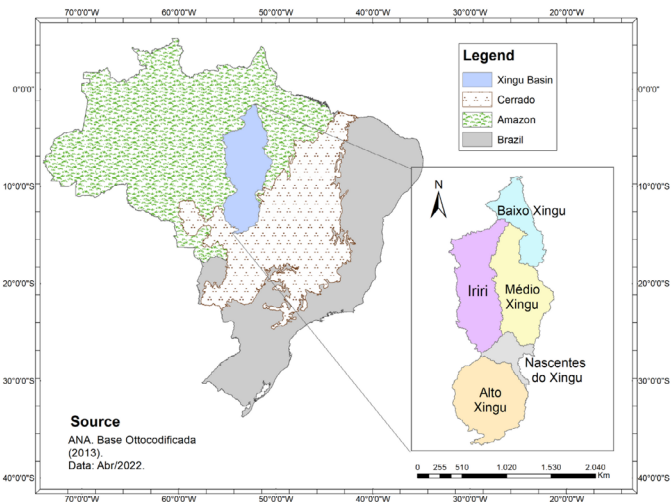


Figure 1 – Geographic boundaries of the biomes belonging to the Xingu basin.

Following this line, the dominant Amazonian vegetation is the so-called dense rainforest characteristic of humid regions with high ET rates, while in the Cerrado there is primacy of low-lying plants with adaptations in storing water for survival in times of drought (Isa, 2012; Santana et al., 2019; Oliveira et al., 2020).

The use and occupation of land in the Xingu basin are predominantly shaped by the economic activities carried out in the region. The main modified land cover activities include soy cultivation, livestock farming, and pastures, which are prevalent in the southern portion of the basin, corresponding to the Mato Grosso region. Cocoa cultivation, the wood extractive industry, and other agricultural crops dominate the Amazon portion located in state of Pará (Salati et al., 1983; Klink and Moreira, 2002; Isa, 2016). On macro scales, as observed in the Xingu basin, changes in land cover can influence regional climate, reducing the occurrence of precipitation and consequent decrease in ET (Davidson et al., 2012; Stickler et al., 2013; Silva and Rezende, 2021).

Estimation of real evapotranspiration through remote sensors

Data referring to actual ET were obtained from the combination of six products and two models of remote sensors merged together: MOD16A2 (Running et al., 2017), PML_V2 (Zhang et al., 2019), Terra Climate (Abatzoglou et al., 2018), ERA5-Land (Muñoz-Sabater, 2019), GLEAM_v3.3^a (Martens et al., 2017), SSEBop (Senay et al., 2013), FLUXCOM (Jung et al., 2019), and FLDAS (McNally et al., 2017). The Google Earth Engine (GEE) platform facilitated the comparison of ET predictions pixel by pixel, of all eight sets, excluding inconsistent estimates of individual ET products. Subsequently, the ET products were resampled to a 1km pixel size using the nearest neighbor method. Finally, the outliers were removed, and the new product was reduced by the Normalized Difference Vegetation Index (NDVI), for a resolution of 1km. This grouping gave rise to a single product, spanning the period from 1985 to 2020, generating the Median.

At the same time, land use and land cover data were obtained through the MapBiomas platform (Collection 6), comprising Landsat Thematic Mapper (TM), Enhanced Thematic Mapper Plus (ETM+), and Operational Land Imager (OLI) sensors, on board Landsat 5, Landsat 7, and Landsat 8, respectively. This platform has a direct interface with GEE, allowing the data acquisition methodology to be the same, only with adaptations in the base script, providing information about land cover and use for the same mentioned data range. It is important to highlight that, in order to evaluate the direct influence between the variables, the MapBiomas data set was resampled to a spatial resolution of 1km.

Estimation of land cover and use through MapBiomas

Collection 6 of MapBiomas offers a total of 25 values with corresponding colors and descriptions, categorized into four macro levels of available land cover types converted in this study: forest, agriculture, non-vegetated area, and water (MapBiomas, 2022). In the present study, the coverage variations verified for the Xingu basin were reclassified and grouped into four classes according to the level 1 classification system compatible with the Food and Agriculture Organization of the United Nations (FAO) and the Brazilian Institute of Geography and Statistics (*Instituto Brasileiro de Geografia e Estatística — IBGE*):

- Forest Formation: evergreen forest, featuring enclaves of savannah, natural pastures, and extensive mangroves and surface waters, with nearly 20% of the forest area biome deforested;
- Pasture: dominated by annual herbaceous plants, natural or planted, related to agricultural activity;
- Agricultural Land: areas predominantly occupied by cultivated/planted annual crops;
- Cerrado: Mosaic of Cerrado, field, and forest, 50% of the native vegetation cover has already been converted (*Plano de Ação para Prevenção e Controle do Desmatamento no Bioma* by Instituto Nacional de Pesquisas Espaciais – PPCerrado/Inpe).

For this reason, in order to statistically correlate the data generated from the “Median” product, only the annual ETr values were filtered, coming from the aggregation of the sets MOD16A2, PML_V2, Terra Climate, ERA5-Land, GLEAM_v3.3a, FLUXCOM, SSEBop, FLDAS, and ERA5-Land, in the masks of land cover conversion ranges, produced by MapBiomas: Forest to Pasture; Forest to Agricultural Land; Cerrado to Pasture; Cerrado to Agricultural Land.

Still, in order to correctly estimate ET behavior by climatological period in the Xingu basin, precipitation data were obtained for the same period (1985-2020) within the Xingu basin using the Climate Hazards Group InfraRed Precipitation with Station Data (CHIRPS) dataset, which incorporates infrared satellite imagery from the National Oceanic and Atmospheric Administration’s (NOAA) Geostationary Operational Environmental Satellite (GOES) system, combined with on-site observation data from various sources, including national me-

teorological agencies and non-governmental organizations, in the production of gridded rainfall time series (Funk et al., 2015).

The CHIRPS dataset, available on the GEE platform, is particularly useful for regions with sparse ground station observations. It not only incorporates data from *in loco* stations into the images but is also systematically bias-corrected, resulting in more accurate precipitation estimates (Funk et al., 2015; Liu et al., 2019).

In the context of the data sets used in the present study, Table 1 compiles the information on the characteristics of each product.

Application of statistical methods to measure correlation

The statistical methods used for data processing in the present study involved graphical analyzes of combined dispersion diagrams. For this purpose, the free version of the STASTICA® software was used. This procedure was chosen due to its capability to correlate continuous and qualitative numerical variables, aligning with the present case where ET was defined as the dependent variable, and land cover as the independent one. It is noteworthy that the ET were previously submitted to the Shapiro-Wilk normality test (Shapiro and Wilk, 1965), guaranteeing results with a 90% confidence interval in the considered region.

Graphical analyses play a crucial role in understanding and enhancing the visualization of dataset characteristics. The combined scatter diagrams allow the measurement of the behavior of a given variable. Representing the entire dataset, this approach facilitates decision-making by providing a comprehensive overview of the information. Thus, it was possible to study the annual trend behavior of ET, obtained in four land cover conversion ranges, between 1985 and 2020:

- Forest to Agricultural Land.
- Forest to Pasture.
- Cerrado to Agricultural Land.
- Cerrado to Pasture.

In addition, the annual ET by range of land use conversion underwent the non-parametric Mann-Kendall test (Mann, 1945; Kendall, 1975), through the ProUCL software (EPA, 2015). This software is widely regarded for its application in temporal hydrological data series, in order to evaluate the trend of variation of real ET under transitions in vegetation cover.

Table 1 – Data set and its specifications for calculating evapotranspiration, precipitation, and land cover.

Data Set	Temporal Resolution	Spatial Resolution	Data Period	Source
Median	Monthly	1km	1985-2020	Present Job
Map Biomas	Yearly	1km*	1985-2020	MapBiomas (2022)
CHIRPS	Monthly	5km	1981-present	Funk et al. (2015)

* Resampling of 30m of the original product to 1km.

Positive test values result in increasing trends, while negative values correspond to decreasing trends, always related to the specific significance level. In this work, a significance level of 95% was adopted.

Finally, the analysis corresponding to the annual growth rate was applied to the area values of each of the land use and land cover type, as well as to the corresponding ET data (in mm/month), with a view to characterize trends by comparing the years within the 1985-2020 period. Thus, the variable value in a year was divided by its base value for comparison (corresponding to the previous year), defining the percentage of data variation — increase, decrease, neutrality (Forman, 1999).

Results and Discussion

the land use and land cover dynamics within the Xingu basin, obtained through the crop conversion intervals from MapBiomas Collection 6, are visually depicted in the different portions of the basin (Figure 2). In order to complement the interpretation of land use and land cover variation in the Xingu basin, the contribution area of changes over the period 1985-2020 for each type of land use and land cover was also verified, as shown in Figure 3. The total area of the Xingu basin at the extremes of the study period is provided in Table 2.

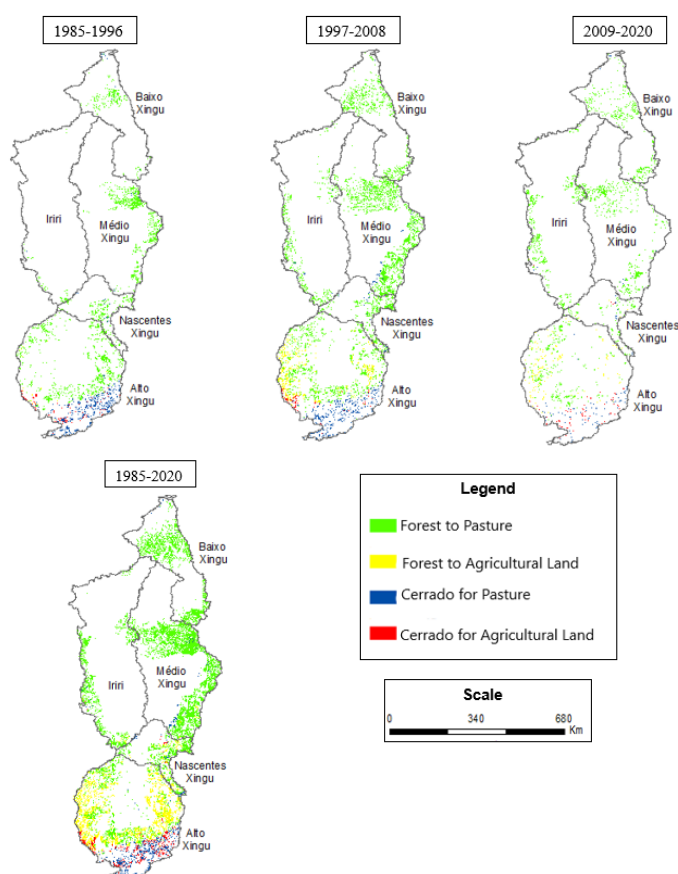


Figure 2 – Annual spatial distribution of changes in land use and land cover for the Xingu basin in the period 1985–2020.

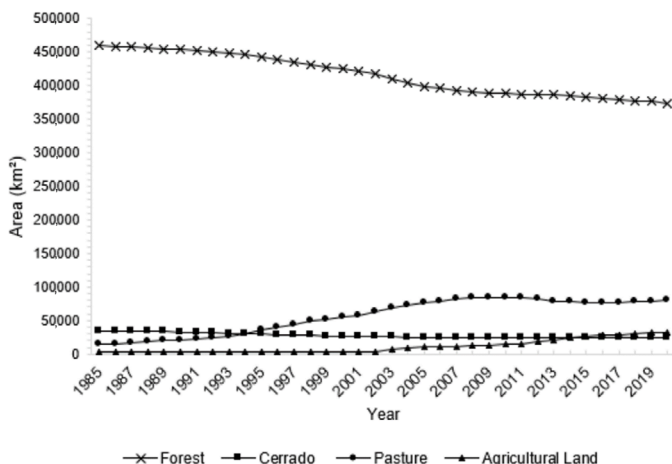


Figure 3 – Variation in land use and land cover in the Xingu basin in the period 1985–2020.

Table 2 – Percentages of land use and cover compared to the Xingu basin area in the period 1985–2020.

Land Use and Coverage Classes	1985		2020	
	Area (km ²)	Percent (%)	Area (km ²)	Percent (%)
Forest	45,394	86.47	373,131	70.24
Cerrado	33,848	6.37	23,931	4.51
Pasture	14,590	2.75	81,092	15.26
Agricultural Area	3,589	0.68	32,846	6.18

To start the assessments, the maps shown in Figure 2 illustrate the behavior of land use and land cover in each sub-basin component. In the Upper Xingu portion, there is a notable concentration of forest-pasture conversion between 1985 and 1996, with a particular emphasis on savannah-pasture conversion in its southern portion. From 1997 to 2008, transitions from forest and *Cerrado* to agricultural areas have already been identified. Little is observed of an increase in the transitions between 2009–2020, but it is still possible to observe the continuation of the removal of forest and *Cerrado* for pasture. Unlike other sub-basins, the Upper Xingu is characterized by intense soybean cultivation, cattle ranching, and logging, the main causes of soil transformations (Velásquez et al., 2010; Isa, 2012; Saddique et al., 2020). Converging due to its geographical proximity and plant characteristics to the Upper Xingu, the Nascentes do Xingu sub-basin exhibits a similar trend in soil transitions, particularly in the complete period of forest to pasture conversion.

The Middle Xingu, representing a substantial proportion of the Amazon Forrest and *Cerrado* biome conversion vegetation. Stands out as the second sub-basin with the greatest transformation in land use and land cover. Throughout the intervals from 1985 to 2020, there is a prevailing trend of forest removal for pasture areas, as well as in the

Iriri and Baixo Xingu sub-basins. These regions are characterized by robust cattle ranching, followed by cocoa plantations. Only the portion of Baixo Xingu stands out for its intense wood extraction.

In central stretches of the basin, a convergence of some vegetation formations native to the two biomes of the Xingu stands out. The presence of savannah, typically belonging to the *Cerrado*, is distributed in characteristic locations of the Amazon Forest. This occurrence results from the significant degree of kinship between some species of vegetation of the biomes, their genera and families, due to their location in a transitional zone of the formations (Kunz et al., 2009; Cruz et al., 2021). Studies suggest that tropical forests and savannas may have similar ET values in these areas, since both are limited to the same climate and water availability (Rodrigues et al., 2014).

Table 2 provides the percentage of land use and land cover in the Xingu basin during the extreme years of the period (1985–2020). Figure 3 shows the evolution of land use and land cover for the Forest, Pasture, *Cerrado*, and Agricultural Area. The forest class corresponds to the largest territorial coverage of the basin, however, there was a decline of 16.23% over the analyzed period. Although there is conversion of *Cerrado* to pasture or agricultural areas, its decline is substantially smaller compared to forests (-1.86%), starting in 1991. On the other hand, pastures in Xingu increased by approximately +12.51% since 1987, while the expansion of agricultural areas became more significant from 2003 onward, reaching +5.5%.

Over the 30-year period (1985–2020), this study indicates that changes in land use and land cover in the Xingu basin are closely tied to the economic characteristics of the region. The suppression of forest areas may be related to the expansion of pasture areas for cattle ranching and agricultural crop cultivation, such as soybeans (Isa, 2012; Santos et al., 2019).

The conversion of the Amazon and *Cerrado* biomes into pasture or agricultural areas has implications for soil water infiltration rates, actual ET, and favors surface runoff, generating erosion processes and silting of the watercourse gutters. In the Amazon region, deforestation and replacement of vegetation cover by new land uses have a strong influence on the climatic variables of the hydrological cycle (Fu et al., 2013; Oliveira et al., 2020). Specifically, between 2000–2010, the conversion of vegetation into pasture areas and agricultural land resulted in a shift from latent heat fractionation to sensible heat fluxes and a decrease in net surface radiation, contributing to an increase in ET (Blunden et al., 2013; Cabral Júnior et al., 2022).

The use of ET data is valid to identify the behavior of vegetation cover, since ET in the dry season is characterized as a reliable indicator of deforested areas (Fohrer et al., 2001; Yang et al., 2012; Silva et al., 2022). At the same time, it should be considered that, although there are several remote sensor products capable of estimating ET, their spatial resolution, generally moderate to low, as in the case of the present work (1 km), promotes a certain limitation in the comparison between the factors, since it directly affects surface detailing, mainly in conversion areas (Trambauer et al., 2014).

Figure 4 shows the long-term monthly ET behaviors for each land use and land cover transition, in the total period 1985–2020 in the Xingu basin, using the Mann-Kendall trend test.

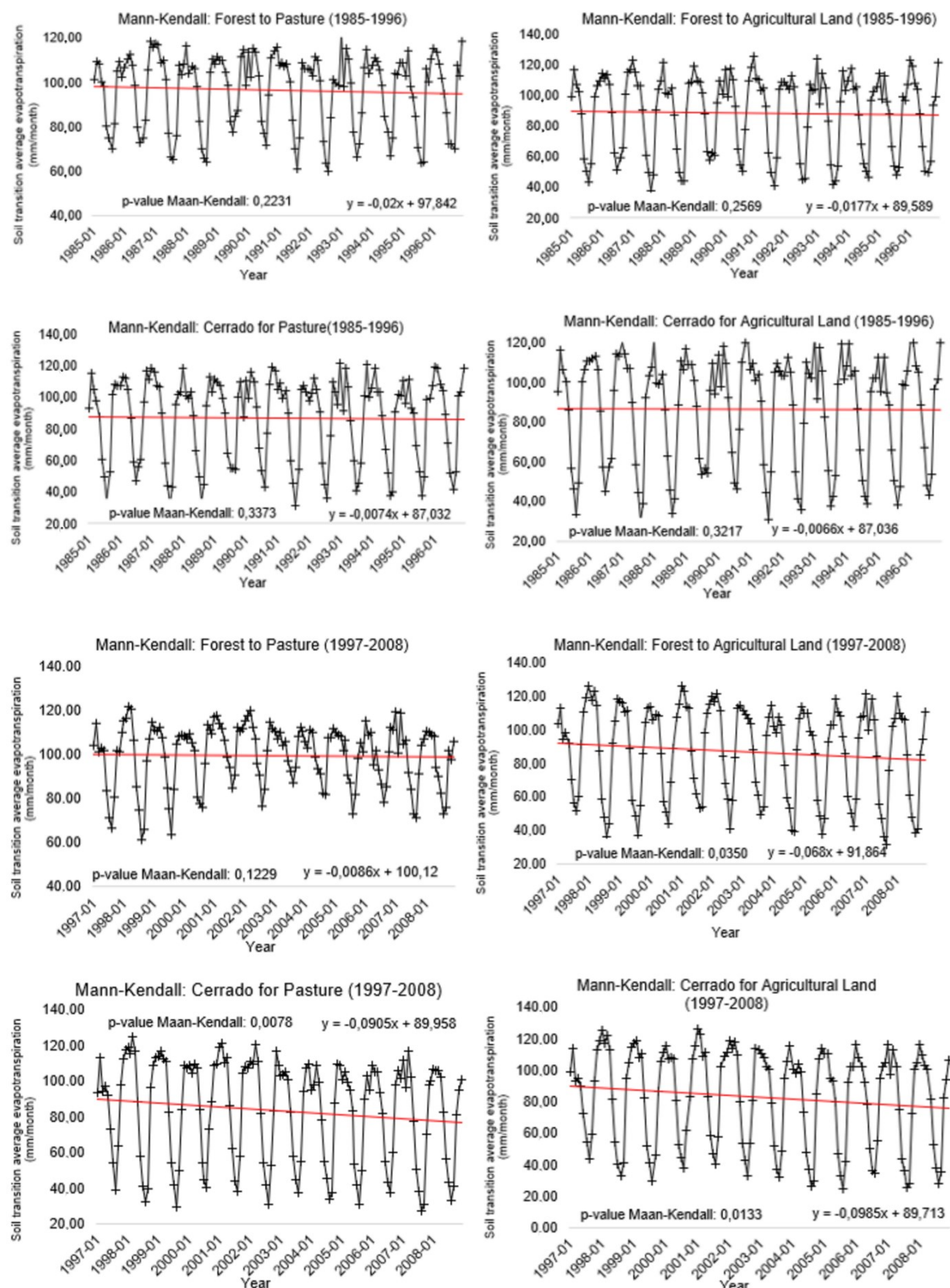


Figure 4 – Trend behavior of real evapotranspiration by conversion of land use in the period 1985–2020

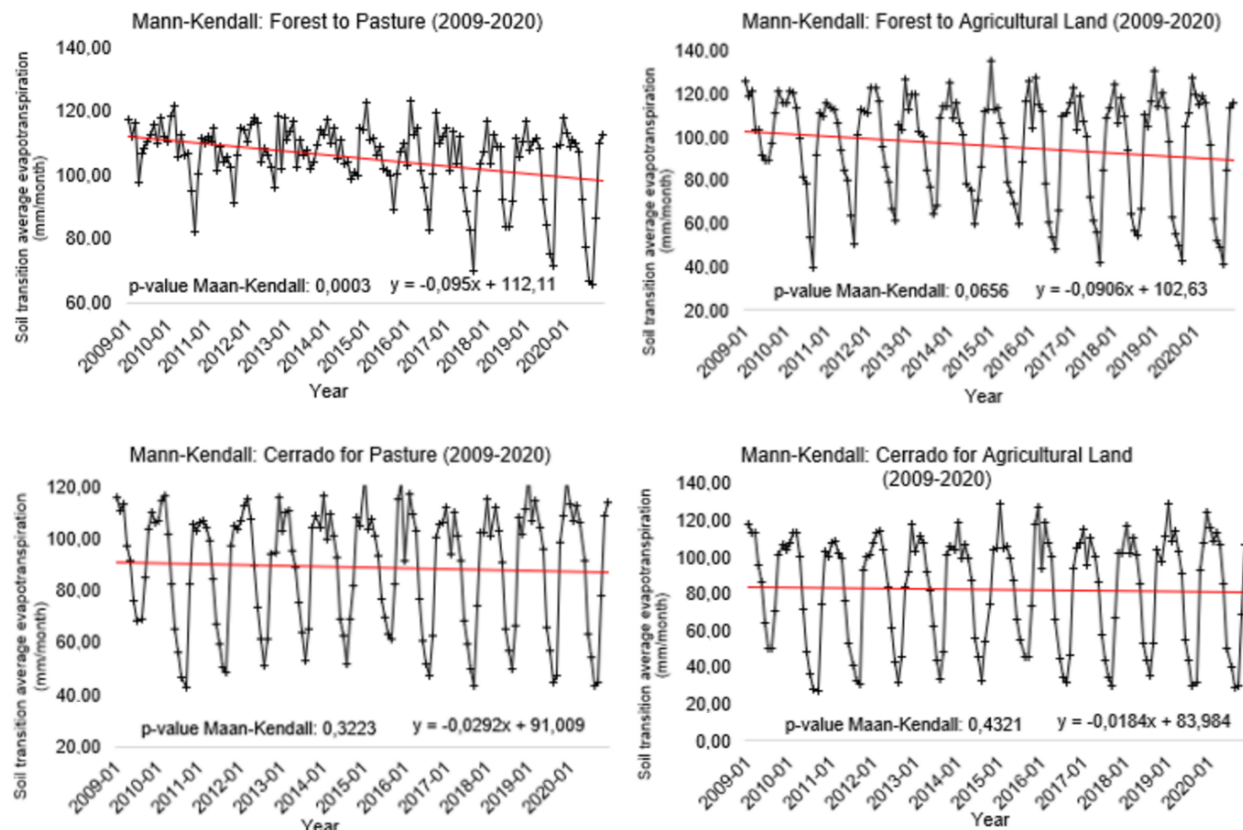


Figure 4 (continue) – Trend behavior of real evapotranspiration by conversion of land use in the period 1985–2020.

According to the graphics in Figure 4, the average monthly variation in ET in each worked period can be derived from the slope of the trend line, based on soil conversion. Notably, the greatest variation corresponded to the change “forest to pasture”, showing a decreasing trend of 0.095 mm/month between 2009–2020, with a significance level of 95%. Then, the conversion “savannah to pasture” shows the second largest decreasing trend in ET (0.090 mm/month between 2009–2020).

In general, the angular coefficients of the equations of the straight lines for each graphic indicate that the transitions of land use cause a trend of monthly decrease in ET across all time intervals, corroborating the statement by Pritchett (1979) that by removing vegetation cover, the average ET tends to be reduced. It is worth noting that ET depends on the crop cycle and variation, due to the significant variations in growth and time that each planting has, from the moment the soil is uncovered until full development (Oliveira et al., 2020; D'Acunha et al., 2024).

The conversion ET graphics of “forest to pasture” (1985–1996; 1997–2008), “forest to agricultural area” (1985–1996), “savannah to pasture” (1985–1996; 2009–2020), and “savannah to agricultural area” (1985–1996; 2009–2020) have p-values greater than 0.05, render-

ing the ET trend statistically non-significant (Mann, 1945; Kendall, 1975). However, it is worth mentioning that in the periods covered in this study, the greatest variations are recorded in the conversion of forest to pasture and/or agricultural area, corroborating the other statistics presented, given the occupation of the area represented by this typology.

The conversion of native vegetation into pastures or agricultural lands directly influences river seasonality, potentially modifying the hydroclimatology of the Xingu river basin. Several studies indicate that the replacement of native vegetation by other land covers increases water production in the basins, positively impacting the hydrological cycle (Dias et al., 2015; Panday et al., 2015; Ivo et al., 2020; Cabral Júnior et al., 2022).

In the case of the Xingu basin, which has the presence of two biomes with very different characteristics in the northern and southern portions of its latitudinal extensions, respectively the Amazon and Cerrado, the distribution of precipitation throughout the year will establish the availability of water for ET. According to the study by Mahrt et al. (2001), ET is also directly proportional to the balance of solar radiation, influenced by light energy that controls stomatal closing and opening in leaf vegetation.

In general, the trends shown in Figure 4 express what was discussed in the study by Calder (1988): the highest ET values coincide with larger soil covers, since they have a more developed root system, and allow an increase in water vapor transfer due to the rough surface of their canopies (during the rainy season).

However, although forests typically present, due to their native characteristics, higher average ET rates, carried out in the Cerrado, during the longest period of the rainy season, described in the months of December to May in the biome, soybean cultivation areas — significant in the Xingu basin — can return higher ET values than native vegetation due to the type of crop maintenance and the distinct seasonal characteristics of the biome, resulting in higher ET rates for agricultural lands compared to forests (Spera et al., 2016; Ivo et al., 2020).

As addressed by Giambellucca et al. (2003), the spatial behavior and intensity of ET in forest fragments within large basins influence deforestation conditions in surrounding areas, unlike small basins, that lack a variety of types of land use associated with intense temporal changes.

With a view to evaluating the behavior of ET from the hydroclimatological stations marked in the basin as a function of the average, precipitation data were obtained, through the CHIRPS satellite, for the Xingu basin in the same period of study: 1985-2020 (Figure 5).

Initially, the graphic in Figure 5 corroborates previous discussions, indicating that in the predominantly forested Xingu basin, ET is proportional to the rainfall index. In the Cerrado region of Mato Grosso, precipitation is concentrated during the hot and humid season: the summer. In this sense, this region tends to lower ET rates, due to the lower potential ET and the effects of deforestation. On the other hand, the portion of the Amazon Forest in the Xingu, located in the state of Pará, experiences well-distributed rainfall throughout the year, with even more expressive rates in the summer, making it more susceptible to significant impacts on ET following vegetation cover removal, especially when potential ET is high due to greater availability of water in the soil (Hewlett and Hibbert, 1967).

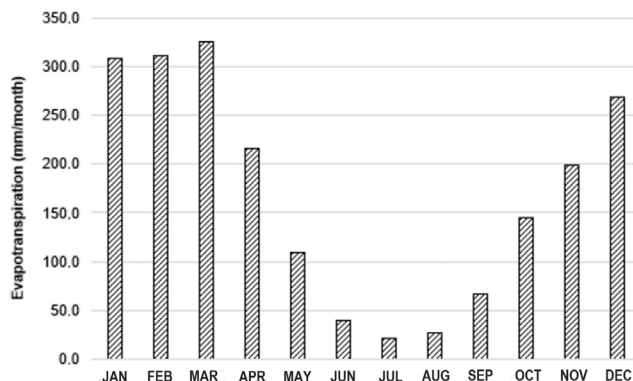


Figure 5 – Monthly long-term average of precipitation in the Xingu basin for the period 1985-2020.

Although there are well-defined plots in both biomes, the conversion vegetation range occupies a large part of the basin, a factor that considerably influences the average ET values in the region (Kunz et al., 2009; Cruz et al., 2021).

The noticeable decrease in ET in 2005, followed by 2010, 2015, and 2016, mirrors the findings in Figure 4. In 2005, the Brazilian Amazon suffered from very low precipitation levels attributed to *El Niño* and positive dipole phenomena in the tropical North Atlantic, affecting cloud formation and consequent rainfall, intensified by persistent fires in the region (Marengo et al., 2008; Tomasella and Marengo, 2011; Papastefanou et al., 2020). On the other hand, in 2010, Marengo et al. (2011) state that there was a marked intensification of the drought, due to the beginning of the austral summer during the *El Niño*, added to the warming in the tropical North Atlantic, corroborated by Brown et al. (2011), Saatchi et al. (2013), Serrão et al. (2017), and Jimenez et al. (2018). However, ET variations in the typology of “forests” did not decrease notably in 2010, likely due to the storage of water in the soil, from previous rainy seasons, which even in times of drought are capable of maintaining high ET rates throughout the interval (Zelazowski et al., 2011; Cabral Júnior et al., 2022).

The spike in deforestation between 2005 and 2010, combined with the severe drought in the Amazon in the same year, exacerbated changes in the water balance (Panday et al., 2015; Caioni, 2021). In the period 2009-2010, precipitation rates in the entire Xingu basin had an increase greater than the climatological normals in the region due to the occurrence of floods caused by the cooling of the North Atlantic Surface Temperature (Caioni, 2021), resulting in higher conversion ET rates as shown in Figure 4.

The drought in the Xingu basin between 2015 and 2016, caused by a moderate to strong *El Niño* and the Intertropical Atlantic Dipole, led to significant decreases in precipitation and flow in the region, disrupting the ET balance, given basin's susceptibility to Atlantic and Pacific Ocean phenomena (CPRM, 2018; Jimenez et al., 2018).

The previous analysis has an intrinsic relationship with the Arch of Deforestation, a region that extends from the west of Maranhão and south of Pará toward the west, passing through Mato Grosso, Rondônia, and Acre, contemplating the center-south of the Xingu basin. Corroborating the assertion, the Xingu comprises one of the most impacted basins in the Brazilian Amazon over the past 50 years, originating primarily from deforestation for agricultural expansion and construction of large works (Isa, 2016).

Following the context, Figure 6 presents the graphs for the periods from December to May (rainy season); from June to September (dry season); and the conversion season between October and November (transition season) (Lucas et al., 2009, 2021).

The analysis presented in Figure 6 provides valuable insights into the relationship, in the dry period, between the conversion of ‘forest to pasture’ and above-average ET patterns.

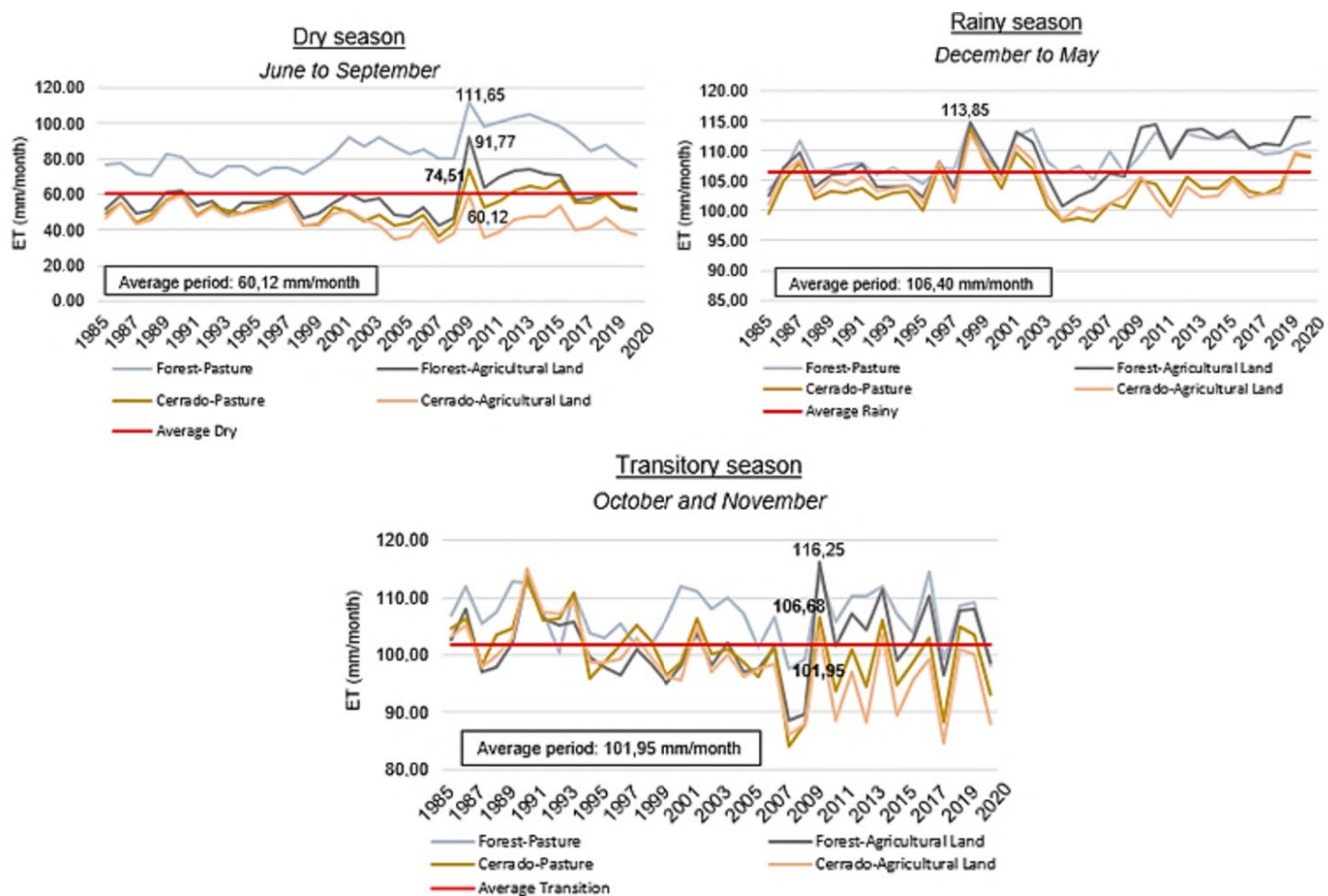


Figure 6 – Behavior of real evapotranspiration by conversion of land use and land cover as a function of hydroclimatological stations in the period 1985–2020.

Still, the data for the dry period differed little from the ET estimates for the rainy period, indicating that even in opposite climatological seasons, the conversion of forests into pastures still produces high ET indices due to the root characteristics of native vegetation, capable of storing water for long periods of time (Maeda et al., 2017), and stomatal control of the seasonal cycle of ET (Costa et al., 2010; O'Connor et al., 2019).

The strong seasonal cycle in the Xingu basin, closely linked to precipitation patterns, is evident in the transitional season. During this period, corresponding to the transition phase from the dry to the rainy season, ET reaches its maximum peak between October and November. This fact can be corroborated, as there is a considerable increase in ET in the second half of the dry season and at the beginning of the rainy season, as also observed in the work by Sun et al. (2019).

Across all three periods, the conversions of “forest to agricultural area” and “savannah to agricultural area” presented variation curves with very similar behavior, considering that these alterations in the vegetation cover alter the dynamics of the soil, but the hydrological demand of the planted crops, especially soybeans in the Xingu basin, promotes small extreme ET fluctuations, driven by the restriction of water in the soil (Alves, 2021; Lucas et al., 2021).

Conclusions

For the 4 land cover classes analyzed through the MapBiomass collection 6, it was possible to associate them with ET in the period 1985–2020, estimated by the product created in this work: “Median”. The largest coverage area in the entire period corresponds to the forest, being also the only one that had a sharp decline in area (about 16.23% of decrease). On the other hand, a high increase in the appearance of pastures was registered in the Xingu, from 1987 onward, in the order of +12.51%, while the growth of agricultural areas increased from 2003, reaching +5.5%. The Alto Xingu sub-basin was the only one to show significant growth in the “savannah-pasture”, “savannah-agricultural area”, and “forest-agricultural area” transitions, while the others concentrate transformations of forests into pastures.

The greatest variations found in ET corresponded to the changes “forest to pasture”, which is characterized by a decreasing trend of 0.095 mm/month, and “savannah to pasture” with the second highest tendency to decrease in ET equal to 0.090 mm/month, both between 2009–2020. The maximum ET peak occurs during the converting season, preceded by an increase in the second half of the dry season, following the beginning of the rainy season.

Authors' contributions

ANTUNES, S.R.C.: conceptualization; data curation; formal analysis; acquisition; investigation; methodology; writing – original draft. RIBEIRO, C.B.M.: project administration; supervision; writing – review & editing. LIMA, R.N.S.: data curation; software; validation; writing – review & editing. GETIRANA, A.: writing – review & editing.

References

- Abatzoglou, J.T.; Dobrowski, S.Z.; Parks, S.A.; Hegewisch, K.C., 2018. Terraclimate, a high-resolution global dataset of monthly climate and climatic water balance from 1958–2015. *Scientific Data*, v. 5, 170191. <https://doi.org/10.1038/sdata.2017.191>
- Alves, E.S.; Rodrigues, L.N.; Cunha, F.F.; Farias, D.B.S., 2021. Evaluation of models to estimate the actual evapotranspiration of soybean crop subjected to different water deficit conditions. *Annals of the Brazilian Academy of Sciences*, v. 93, (4), 1-16. <https://doi.org/10.1590/0001-3765202120201801>
- Blunden, J.; Arndt, D.S.; Achberger, C.; Ackerman, S.; Albanil, A.; Alexander, P.; Alfaro, E.; Allan, R.; Alves, L.M.; Amador, J.A.; Ambenje, P.; Andrianjafinirina, S.; Antonov, J.; Aravéquia, J.A.; Arendt, A.; Arevalo, J.; Ashik, I.; Atheru, Z.; Banzon, V.; Baringer, M.O.; Barreira, S.; Barriopedro, D.; Beard, G.; Becker, A.; Behrenfeld, M.J.; Bell, G.D.; Benedetti, A.; Bernhard, G.; Berrisford, P.; Berry, D.I.; Bhatt, U.S.; Bidegain, M.; Bindoff, N.L.; Bissolli, P.; Blake, E.S.; Booneeady, R.; Bosilovich, M.; Box, J.E.; Boyer, T.; Braatzen, G.; Bromwich, D.H.; Brown, R.; Bruhwiler, L.; Bulygina, O.N.; Burgess, D.; Burrows, J.; Calderon, B.; Camargo, S.J.; Campbell, J.; Cao, Y.; Cappelen, J.; Carrasco, G.; Chambers, D.P.; Chang'a, L.; Pearce, P.; Chehade, W.; Chelliah, M.; Christiansen, H.H.; Christy, J.R.; Ciais, P.; Coelho, C.A.S.; Cogley, J.G.; Colwell, S.; Cross, J.N.; Crouch, J.; Cunningham, S.; Dacic, M.; de Jeu, R.; Dekka Francis, S.; Demircan, M.; Derksen, C.; Diamond, H.J.; Dlugokencky, E.J.; Dohan, K.; Dolman, H.; Domingues, C.M.; Dong, S.; Dorigo, W.A.; Drozdov, D.S.; Dugay, C.; Dunn, R.J.H.; Durán-Quesada, A.M.; Dutton, G.S.; Ehmann, C.; Elkins, J.W.; Euscategui, C.; Famiglietti, J.S.; Fan, F.; Fauchereau, N.; Feely, R.; Fekete, B.M.; Fenimore, C.; Fioletov, V.E.; Fogarty, C.; Fogt, R.L.; Folland, C.K.; Foster, M.J.; Frajka-Williams, E.; Franz, B.A.; Frith, S.; Frolov, I.Y.; Ganter, C.; Garzoli, S.L.; Geai, M.-L.; Gerland, S.; Gitau, W.; Gleason, K.L.; Gobron, N.; Goldenberg, S.B.; Goni, G.; Good, S.A.; Gottschalck, J.; Gregg, M.C.; Griffiths, G.; Grooss, J.-U.; Guard, C.; Gupta, S.K.; Hall, B.D.; Halpert, M.S.; Harada, Y.; Hauri, C.; Heidinger, A.K.; Heikkilä, A.; Heim, R.R.; Heimbach, P.; Hidalgo, H.; Hilburn, K.; Ho, S.-P.; Hobbs, W.; Holgate, S.; Hovsepyan, A.; Hu, Z.-Z.; Hughes, P.; Hurst, D.F.; Ingvaldsen, R.B.; Inness, A.; Jaimes, E.; Jakobsson, M.; Adamu, J.; Jeffries, M.O.; Johns, W.E.; Johnsen, B.; Johnson, G.C.; Johnson, B.; Jones, L.T.; Jumaux, G.; Kabidi, K.; Kaiser, J.W.; Kamga, A.; Kang, K.-K.; Kanzow, T.; Kao, H.-Y.; Keller, L.M.; Kennedy, J.J.; Key, J.R.; Khatiwala, S.; Kheyrollah Pour, H.; Kholodov, A.; Khoshkam, M.; Kijazi, A.L.; Kikuchi, T.; Kim, B.M.; Kim, S.-J.; Kimberlain, T.B.; Knaff, J.A.; Korshunova, N.N.; Koskelo, T.; Kousky, V.E.; Kramarova, N.; Kratz, D.P.; Krishfield, R.; Kruger, A.C.; Kruk, M.C.; Kumar, A.; Lagerloef, G.S.E.; Lakkala, K.; Lander, M.A.; Landsea, C.W.; Lankhorst, M.; Laurila, T.; Lazzara, M.A.; Lee, C.; Leuliette, E.; Levitus, S.; L'Heureux, M.; Lieser, J.; Lin, I.-I.; Liu, Y.Y.; Liu, Y.; Lobato-Sánchez, R.; Locarnini, R.; Loeb, N.G.; Loeng, H.; Long, C.S.; Lorrey, A.; Luhunga, P.M.; Lumpkin, R.; Luo, J.-J.; Lyman, J.M.; Macdonald, A.M.; Maddux, B.C.; Malekela, C.; Manney, G.L.; Marchenko, S.; Marengo, J.A.; Marotzke, J.; Marra, J.J.; Martinez-Gueingla, R.; Massom, R.; Mathis, J.T.; McBride, C.; McCarthy, G.D.; McVicar, T.; Mears, C.; Meier, W.; Meinen, C.S.; Menendez, M.; Merrifield, M.A.; Mitchard, E.; Mitchum, G.; Montzka, S.A.; Morcrette, J.-J.; Mote, T.; Mühlé, J.; Mühr, B.; Mullan, B.; Müller, R.; Nash, E.R.; Nerem, R.S.; Newlin, M.L.; Newman, P.; Ng'ongolo, H.; Nieto, J.J.; Nishino, S.; Nitsche, H.; Noetzli, J.; Oberman, N.G.; Obregon, A.; Ogalo, L.; Oludhe, C.S.; Omar, M.I.; Overland, J.E.; Oyunjargal, L.; Parinussa, R.; Park, G.-H.; Park, E.-H.; Parker, D.; Pasch, R.J.; Pascual-Ramirez, R.; Pelto, M.; Penalba, O.; Peng, L.; Perovich, D.K.; Pezza, A.B.; Phillips, D.; Pickart, R.; Pinty, B.; Pitts, M.C.; Purkey, S.G.; Quegan, S.; Quintana, J.; Rabe, B.; Rahimzadeh, F.; Raholiao, N.; Raiva, I.; Rajeevan, M.; Ramiandrisoa, V.; Ramos, A.M.; Ranivoarisoa, S.; Rayner, N.A.; Rayner, D.; Razuveav, V.N.; Reagan, J.; Reid, P.A.; Renwick, J.A.; Revedekar, J.; Richter-Menge, J.; Rivera, I.L.; Robinson, D.; Rodell, M.; Romanovsky, V.E.; Ronchail, J.; Rosenlof, K.H.; Sabine, C.L.; Salvador, M.A.; Sanchez-Lugo, A.; Santee, M.L.; Sasgen, I.; Sawaengphokhai, P.; Sayouri, A.; Scambos, T.; Schauer, U.; Schemm, J.; Schlosser, P.; Schmid, C.; Schreck, C.J.III; Semiletov, I.P.; Send, U.; Sensoy, S.; Setzer, A.W.; Severinghaus, J.; Shakhova, N.; Sharp, M.J.; Shiklomanov, N.; Siegel, D.A.; Silva, V.C.B.; Silva, F.D.S.; Sima, F.; Simeonov, P.; Simmonds, I.; Simmons, A.; Skansi, M.M.; Smeed, D.; Smethie, W.M.; Smith, A.; Smith, C.; Smith, S.L.; Smith, T.M.; Sokolov, V.; Srivastava, A.K.; Stackhouse Jr, P.W.; Stammerjohn, S.; Steele, M.; Steffen, K.; Steinbrecht, W.; Stephenson, T.S.; Su, J.; Svendby, T.M.; Sweet, W.V.; Takahashi, T.; Tanabe, R.M.; Taylor, M.A.; Tedesco, M.; Teng, W.; Thépaut, J.-N.; Thiaw, W.M.; Thoman, R.; Thompson, P.R.; Thorne, P.W.; Timmermans, M.-L.; Tobin, S.; Toole, J.; Trewin, B.C.; Trigo, R.M.; Trotman, A.; Tschudi, M.A.; Van de Wal, R.S.W.; Van der Werf, G.R.; Vazquez, J.L.; Vieira, G.; Vincent, L.; Vose, R.S.; Wagner, W.; Wahr, J.; Walsh, J.; Wang, J.; Wang, C.; Wang, M.; Wang, S.-H.; Wang, L.; Wanninkhof, R.; Weaver, S.; Weber, M.; Werdell, J.; Whitewood, R.; Wijffels, S.; Wilber, A.; Wild, J.; Willett, K.M.; Williams, W.; Willis, J.; Wolken, G.J.; Wong, T.; Woodgate, R.; Worthy, D.E.J.; Wouters, B.; Wovrosch, A.J.; Yan, X.; Yamada, R.; Zungang, Y.; Yu, L.; Zhang, P.; Zhao, L.; Zhong, W.; Ziemke, J.R.; Zimmermann, S., 2013. State of the Climate in 2012. *Bulletin of the American Meteorological Society*, v. 94, (8), S1-S238. <https://doi.org/10.1175/2013BAMSStateoftheClimate.1>
- Brown, F.; Santos, G.P.; Pires, F.F.; Costa, C.B., 2011. Brazil: Drought and Fire Response in the Amazon. *World Resources Report Case Study*, Washington DC.
- Cabral Júnior, J.B.; da Silva, H.J.F.; dos Reis, J.S., 2022. Características da Cobertura do Solo em Anos de Contrastes Climáticos (chuvisco e seco) no Oeste da Amazônia, Rio Branco – Acre. *Revista Brasileira De Geografia Física*, v. 15, (6), 2704-2714. <https://doi.org/10.26848/rbgf.v15.6.p2704-2714>
- Caioni, C., 2021. Efeito da seca sobre o balanço hídrico na bacia do rio Xingu. *Agrarian Academy*, v. 8, (15), 40-53.
- Calder, I.R., 1998. Water-resource and land-use issues. SWIM Paper 3. International Water Management Institute, Colombo, Sri Lanka.
- Costa, M.H.; Foley, J.A., 2000. Combined effects of deforestation and doubled atmospheric CO₂ concentrations on the climate of Amazonia. *Journal of Climate*, v.13, (1), 18-34. [https://doi.org/10.1175/1520-0442\(2000\)013<0018:CEODAD>2.0.CO;2](https://doi.org/10.1175/1520-0442(2000)013<0018:CEODAD>2.0.CO;2)
- Costa, M.H.; Biajoli, M.C.; Sanches, L.; Malhado, A.C.M.; Hutyra, L.R.; da Rocha, H.R.; Aguiar, R.G.; de Araújo, A.C., 2010. Atmospheric versus vegetation controls from Amazonian rainforest evapotranspiration: are wet and seasonally dry forests different? *Journal of Geophysical Research: Biogeosciences*, v. 115, 1-9. <https://doi.org/10.1029/2009JG001179>
- Companhia de Pesquisa de Recursos Minerais (CPRM), 2018. Climatologia da precipitação na bacia hidrográfica do Rio Xingu (Accessed February 23, 2021) at: http://www.cprm.gov.br/sace/conteudo/xingu_artigos/climatologia_xingu.pdf.
- Cruz, W.J.A.D.; Marimon, B.S.; Marimon Junior, B.H.; Amorim, I.; Morandi, P.S.; Phillips, O.L., 2021. Functional diversity and regeneration traits of tree

- communities in the Amazon-Cerrado transition. *Flora*, v. 285. https://doi.org/10.1016/j.flora.2021.151952
- Cunha, Z.A.; Mello, C.R.; Beskow, S.; Vargas, M.M.; Guzman, J.A.; Moura, M.M., 2023. A modeling approach for analyzing the hydrological impacts of the agribusiness land-use scenarios in an Amazon Basin. *Land*, v. 12, (7), 1422. https://doi.org/10.3390/land12071422
- D'Acunha, B.; Dalmagro, H.J.; Zanella de Arruda, P.H.; Biudes, M.S.; Lathuillière, M.J.; Uribe, M.; Couto, E.G.; Brando, P.M.; Vourlitis, G.; Johnson, M.S., 2024. Changes in evapotranspiration, transpiration and evaporation across natural and managed landscapes in the Amazon, Cerrado and Pantanal biomes. *Agricultural and Forest Meteorology*, v. 346, 109875. https://doi.org/10.1016/j.agrformet.2023.109875
- Davidson, E.A.; de Araújo, A.C.; Artaxo, P.; Balch, J.K.; Brown, I.F.; Bustamante, M.M. C.; Coe, M.T.; DeFries, R.S.; Keller, M.; Longo, M.; Munger, J. W.; Schroeder, W.; Soares-Filho, B.S.; Souza, C.M.; Wofsy, S.C., 2012. The Amazon basin in transition. *Nature*, v. 481, 321-328. https://doi.org/10.1038/nature10717
- Dias, L.C.P.; Macedo, M.N.; Costa, M.H.; Coe, M.T.; Neill, C., 2015. Effects of land cover change on evapotranspiration and small basin flow reservoirs in the Upper Xingu River Basin, Brazil Central. *Journal of Hydrology Regional Studies* 4, Part B(PB), 108-122. https://doi.org/10.1016/j.ejrh.2015.05.010
- Environmental Protection Agency (EPA), 2015. ProUCL Version 5.1.002: Technical Guide, Statistical Software for Environmental Applications for Data Sets with and without Nondetect Observations. Publication nº EPA/600/R-07/041. Office of Research and Development, Washington, DC.
- Paramhos Filho, A.C.; Moreira, E.S.; Oliveira, A.K.M. de; Pagotto, T.C.S.; Mioto, C.L., 2014. Análise da variação da cobertura do solo no Pantanal de 2003 a 2010 através de sensoriamento remoto. *Engenharia Sanitária e Ambiental*, v. 19, (spe), 69-76. https://doi.org/10.1590/S1413-41522014019010000305
- Fohrer, N.; Haverkamp, S.; Eckhardt, K.; Frede, H.-G., 2001. Hydrologic response to land use changes on the catchment scale. *Physics and Chemistry of the Earth, Part B: Hydrology, Oceans and Atmosphere*, v. 26, (7-8), 577-582. https://doi.org/10.1016/S1464-1909(01)00052-1
- Forman, R.T., 1999. Land Mosaics: the ecology of landscapes and regions. 5. ed. Cambridge University Press, Cambridge.
- Fu, R.; Yin, L.; Li, W.; Myneni, R.B., 2013. Increased dry-season length over southern Amazonia in recent decades and its implication for future climate. *Proceedings of the National Academy of Sciences of the United States of America*, v. 110, (45), 18110-18115. https://doi.org/10.1073/pnas.1302584110
- Funk, C.; Peterson, P.; Landsfeld, M.; Pedreros, D.; Verdin, J.; Shukla, S.; Husak, G.; Rowland, J.; Harrison, L.; Hoell, A.; Michaelsen, J., 2015. The climate hazards infrared precipitation with stations - a new environmental record for monitoring extremes. *Scientific Data*, v. 2, 150066. https://doi.org/10.1038/sdata.2015.66
- Galina, A.B.; Ilha, D.B.; Pagotto, M.A., 2022. Dinâmica multitemporal da cobertura e uso do solo do estado de Sergipe. *Scientia Plena*, v. 18, n. 6. https://doi.org/10.14808/sci.plena.2022.065301
- Giambelluca, T.W.; Ziegler, A.D.; Nullet, M.A.; Truong, D.M.; Tran, L.T., 2003. Transpiration in a small tropical forest patch. *Agricultural and Forest Meteorology*, v. 117, 1-22. https://doi.org/10.1016/S0168-1923(03)00041-8
- Griffiths, P.; Jakimow, B.; Hostert, P., 2018. Reconstruindo a dinâmica do desmatamento anual de longo prazo no Pará e Mato Grosso usando o arquivo Landsat. *Sensoriamento Remoto do Meio Ambiente*, v. 216, 497-513. https://doi.org/10.1016/j.rse.2018.07.010
- Hayhoe, S.J.; Neill, C.; Porder, S.; McHorney, R.; Lefebvre, P.; Coe, M.T.; Elsenbeer, H.; Krusche, A.V., 2011. Conversion to soy on the Amazonian agricultural frontier increases streamflow without affecting stormflow dynamics. *Global Change Biology*, v. 17, (5), p. 1821-1833. https://doi.org/10.1111/j.1365-2486.2011.02392.x
- Hewlett, J.D.; Hibbert, E., 1967. Factors affecting the response of small watersheds to precipitation in humid areas. In: Sopper, W.E.; Lull, H.W. (Eds.). *International Symposium on Forest Hydrology*. Pergamon Press, Oxford, pp. 275-290.
- Instituto Socioambiental (ISA), 2012. De olho na Bacia do Xingu (Série Cartão Brasil Socioambiental, v. 5).
- Instituto Socioambiental (ISA), 2016. De olho no Xingu: histórico de desmatamento e tendências atuais. *Cartão Brasil Socioambiental*, Parte I.
- Ivo, I.O.; Biudes, M. S.; Vourlitis, G.L.; Machado, N.G.; Martim, C.C., 2020. Effect of fires on biophysical parameters, energy balance and evapotranspiration in a protected area in the Brazilian Cerrado. *Remote Sensing Applications: Society and Environment*, v. 19, 100342. https://doi.org/10.1016/j.rsase.2020.100342
- Jimenez, J.C.; Barichivich, J.; Mattar, C.; Takahashi, K.; Santamaría-Artigas, A.; Sobrino, J.A.; Malhi, Y., 2018. Spatiotemporal patterns of thermal anomalies and drought over tropical forests driven by recent extreme climatic anomalies. *Philosophical Transactions of the Royal Society of London. Series B, Biological Sciences*, v. 373, (1760), 20170300. https://doi.org/10.1098/rstb.2017.0300
- Jung, H.C.; Getirana, A.; Arsenault, K.R.; Holmes, T.R.H.; McNally, A., 2019. Uncertainties in evapotranspiration estimates over West Africa. *Remote Sensing*, v. 11, (8), 892. https://doi.org/10.3390/rs11080892
- Kendall, M.G., 1975. Rank Correlation Methods. 4. ed. Charles Griffin, London.
- Klink, C.A.; Moreira, A.G., 2002. Past and current human occupation, and land use. In: Oliveira, P.S.; Marquis, R.J. *The Cerrado of Brazil: ecology and natural history of a neotropical Savanna*. Columbia University Press, New York, pp. 69-88.
- Kohler, M.R.; Bampi, A.C.; da Silva, C.A.F.; Arantes, A.; Gaspar, W.J., 2021. Desmatamento na Amazônia brasileira sob a ótica da pecuária: a degradação dos recursos hídricos no contexto da região norte do Mato Grosso. *Research, Society and Development*, v. 10, (11), e66101119252. http://dx.doi.org/10.33448/rsd-v10i11.19252
- Kunz, S.H.; Ivanauskas, N.M.; Martins, S.V.; Silva, E.; Stefanello, D., 2009. Análise da semelhança florística entre as florestas do Alto Rio Xingu, da Bacia Amazônica e do Planalto Central. *Brazilian Journal of Botany*, v. 32, (4), 725-736. https://doi.org/10.1590/S0100-84042009000400011
- Liu, J.; Shangguan, D.; Liu, S.; Ding, Y.; Wang, S.; Wang, X., 2019. Evaluation and comparison of CHIRPS and MSWEP daily-precipitation products in the Qinghai-Tibet Plateau during the period of 1981-2015. *Atmospheric Research*, v. 230, 104634. https://doi.org/10.1016/j.atmosres.2019.104634
- Lucas, E.W.M.; Sousa, F.A.S.; Silva, F.D.D.S.; Lucio, P.S., 2009. Variação espacial e temporal da precipitação na bacia hidrográfica do Xingu, Pará. *Revista Brasileira de Meteorologia*, v. 24, (3), 308-322.
- Lucas, E.W.M.; Sousa, F.A.S.; Silva, F.D.D.S.; Rocha Júnior, R.L.D.; Pinto, D.D.C.; Silva, V.P.R., 2021. Trends in climate extreme indices assessed in the Xingu river basin - Brazilian Amazon. *Weather and Climate Extremes*, v. 31, 100306. https://doi.org/10.1016/j.wace.2021.100306
- Maeda, E.E.; Ma, X.; Wagner, F.H.; Kim, H.; Oki, T.; Eamus, D.; Huete, A., 2017. Evapotranspiration seasonality across the Amazon Basin. *Earth System Dynamics*, v. 8, (2), 439-454. https://doi.org/10.5194/esd-8-439-2017

- Mahrt, L.; Vickers, D.; Nakamura, R.; Soler, M.R.; Sun, J.; Burns, S.P.; Lenschow, D.H., 2001. Shallow drainage flows. *Boundary-Layer Meteorology*, v. 101, (2), 243-260. <https://doi.org/10.1023/A:1019273314378>
- Mann, H.B., 1945. Non-parametric tests against trend. *Econometrica*, v. 13, (3), 245-259. <https://doi.org/10.2307/1907187>
- MapBiomas (Org.), 2022. MapBiomas General "Handbook": Algorithm Theoretical Basis Document (ATBD) - Colection 6 (Accessed March 30, 2022) at: https://mapbiomas-br-site.s3.amazonaws.com/Metodologia/ATBD_Collection_6_v1_January_2022.pdf
- Marengo, J.A.; Nobre, C.A.; Tomasella, J.; Oyama, M.D.; Oliveira, G.S.; Oliveira, R.; Camargo, H.; Alves, L.M.; Brown, I.F., 2008. The drought of Amazônia in 2005. *Journal of Climate*, v. 21, 495-516. <https://doi.org/10.1175/2007JCLI1600.1>
- Marengo, J.A.; Tomasella, J.; Alves, L.M.; Soares, W.R.; Rodriguez, D.A., 2011. The drought of 2010 in the context of historical droughts in the Amazon region. *Geophysical Research Letters*, v. 38, (12), 1-5. <https://doi.org/10.1029/2011GL047436>
- Marinho Junior, J.L.; Lima, D.S.; Dias, J.L.A.; Araújo Filho, R.N., 2020. Análise dos estoques de carbono no solo sob diferentes coberturas vegetais no Brasil. *Journal of Biotechnology and Biodiversity*, v. 8, (1), 031-040. <https://doi.org/10.20873/jbb.uft.cemaf.v8n1.marinhojr>
- Martens, B.; Miralles, D.G.; Lievens, H.; van der Schalie, R.; de Jeu, R.A.M.; Fernández-Prieto, D.; Beck, H.E.; Dorigo, W.A.; Verhoest, N.E.C., 2017. GLEAM v3: satellite-based land evaporation and root-zone soil moisture. *Geoscientific Model Development*, v. 10, (5), 1903-1925. <https://doi.org/10.5194/gmd-10-1903-2017>
- McNally, A.; Arsenault, K.; Kumar, S.; Shukla, S.; Peterson, P.; Wang, S.; Funk, C.; Peters-Lidard, C.D.; Verdin, J.P., 2017. A land data assimilation system for sub-Saharan Africa food and water security applications. *Scientific Data*, v. 4, 170012. <https://doi.org/10.1038/sdata.2017.12>
- Muñoz-Sabater, J., 2019. ERA5-Land monthly averaged data from 1981 to present. Copernicus Climate Change Service (C3S) Climate Data Store (CDS).
- Nóbrega, R.S., 2014. Impactos do desmatamento e de mudanças climáticas nos recursos hídricos na Amazônia ocidental utilizando o modelo SLURP. *Revista Brasileira de Meteorologia*, v. 29, (spe), 111-120. <https://doi.org/10.1590/0102-778620130024>
- O'Connor, J.; Santos, M.J.; Rebel, K.T.; Dekker, S.C., 2019. The influence of water table depth on evapotranspiration in the Amazon arc of deforestation. *Hydrology and Earth System Sciences*, v. 23, (9), 3917-3931. <https://doi.org/10.5194/hess-23-3917-2019>
- Oliveira, G.; Chen, J.M.; Mataveli, G.A.V.; Chaves, M.E.D.; Rao, J.; Sternberg, M.; dos Santos, T.V.; dos Santos, C.A.C., 2020. Evapotranspiration and Precipitation over Pasture and Soybean Areas in the Xingu River Basin, an Expanding Amazonian Agricultural Frontier. *Agronomy*, v. 10, (8), 1112. <https://doi.org/10.3390/agronomy10081112>
- Paiva, K.; Rau, P.; Montesinos, C.; Lavado-Casimiro, W.; Bourrel, L.; Frappart, F., 2023. Hydrological response assessment of land cover change in a Peruvian Amazonian Basin impacted by deforestation using the SWAT model. *Remote Sensing*, v. 15, (24), 5774. <https://doi.org/10.3390/rs15245774>
- Panday, P.; Coe, M.T.; Macedo, M.N.; Lefebvre, P.; Castanho, A.D.A., 2015. Deforestation offsets changes in water balance due to climate variability in the Xingu River in eastern Amazon. *Journal of Hydrology*, v. 523, (7), 822-829. <https://doi.org/10.1016/j.jhydrol.2015.02.018>
- Papastefanou, P.; Zang, C.S.; Angelov, Z.; de Castro, A.A.; Jimenez, J.C.; De Rezende, L.F.C.; Ruscica, R.; Sakschewski, B.; Sörensson, A.; Thonicke, K.;
- Vera, C.; Viovy, N.; Von Randow, C.; Rammig, A., 2020. Quantifying the spatial extent and intensity of recent extreme drought events in the Amazon rainforest and their impacts on the carbon cycle. *Biogeosciences Discussions*, p. 1-37. <https://doi.org/10.5194/bg-2020-425>
- Pongratz, J.; Bounoua, L.; DeFries, R.S.; Morton, D.C.; Anderson, L.O.; Mauser, W.; Klink, C.A., 2006. The Impact of Land Cover Change on Surface Energy and Water Balance in Mato Grosso, Brazil. *Earth Interactions*, v. 10, (19), 1-19. <https://doi.org/10.1175/EI176.1>
- Pritchett, W.L., 1979. Properties and Management of Forest Soils. John Wiley, New York, 500 p.
- Rede Xingu+, 2021. Xingu sob Bolsonaro: Análise do desmatamento na Bacia do Rio Xingu (2018-2020) (Accessed May 14, 2021) at: https://www.socioambiental.org/sites/blog.socioambiental.org/files/nsa/arquivos/nt_xingu_sob_bolsonaro_final.pdf
- Rizzo, R.; Garcia, A.S.; Vilela, V.M.F.N.; Ballester, M.V.R.; Neill, C.; Victoria, D.C.; da Rocha, H.R.; Coe, M.T., 2020. Land use changes in Southeastern Amazon and trends in rainfall and water yield of the Xingu River during 1976–2015. *Climatic Change*, v. 162, 1419-1436. <https://doi.org/10.1007/s10584-020-02736-z>
- Rodrigues, T.R.; Vourlitis, G.L.; Lobo, F.A.; Oliveira, R.G.; Nogueira, J.S., 2014. Seasonal variation in energy balance and canopy conductance for a tropical savanna ecosystem in south-central Mato Grosso, Brazil. *Journal of Geophysical Research: Biogeosciences*, v. 119, (1), 1-13. <https://doi.org/10.1002/2013JG002472>
- Rodrigues, T.; Sano, E.E.; Almeida, T.; Chaves, J.M.; Doblas, J., 2019. Detecção de mudanças na cobertura vegetal natural do Cerrado por meio de dados de radar (Sentinel1A). *Sociedade e Natureza*, v. 31, 1-22. <https://doi.org/10.14393/SN-v31-2019-46315>
- Rosatto, A.A.P.; Kirchner, J.H.; Martins, J.D.; Sander, L.S.; Amaral, W.N.B.; Petry, M.T., 2022. Partição da evapotranspiração da cultura da soja em diferentes cultivares em cada estádio fenológico. *IRRIGA*, v. 27, (3), 477-492. <https://doi.org/10.15809/irriga.2022v27n3p477-492>
- Rothmund, L.D.; Almeida Júnior, E.S.; de Arruda Lima, L.P.; Bodnar Massad, H.A.; Palácios, R.S.; Biudes, M.S.; Machado, N.G.; Nogueira, J.S., 2019. Impacto da alteração da cobertura do solo nos parâmetros biofísicos no sul da Floresta Amazônica por sensoriamento remoto. *Revista Brasileira de Climatologia*, v. 25, 122-137. <https://doi.org/10.5380/abclima.v25i0.62677>
- Running, S.; Mu, Q.; Zhao, M., 2017. Mod16a2 Modis/Terra Net Evapotranspiration 8-Day L4 Global 500m Sin Grid V006. NASA EOSDIS Land Processes DAAC, 6.
- Saatchi, S.; Asefi-Najafabady, S.; Malhi, Y.; Nemani, R., 2013. Persistent effects of a severe drought on Amazonian forest canopy. *Proceedings of the National Academy of Sciences of the United States of America*, v. 110, (2), 565-570. <https://doi.org/10.1073/pnas.1204651110>
- Saddique, N.; Mahmood, T.; Bernhofer, C., 2020. Quantifying the impacts of land use/land cover change on the water balance in the afforested River Basin, Pakistan. *Environmental Earth Sciences*, v. 79, (19), 448. <https://doi.org/10.1007/s12665-020-09206-w>
- Sala, O.E.; Chapin, F.S. III; Armesto, J.J.; Berlow, E.L.; Bloomfield, J.B.; Dirzo, R.H.; Huber-Sannwald, E.; Huenneke, L.; Jackson, R.B.; Kinzig, A.P.; Leemans, R.; Lodge, D. M.; Mooney, H.A.; Oesterheld, M.I.N.; Poff, N.L.; Sykes, M.T.; Walker, B.; Walker, M.; Wall, D.H., 2000. Global biodiversity scenarios for the year 2100. *Science*, v. 287, (5459), 1770-1774. <https://doi.org/10.1126/science.287.5459.1770>
- Salati, E.; Shubart, H.; Junk, W., 1983. Amazônia, desenvolvimento, integração, ecologia. Editora Brasiliense, CNPq, São Paulo, 327 p.

- Santana, N.C.; Carvalho Júnior, O.A.; Gomes, R.A.T.; Guimarães, R.F., 2019. Análise do ângulo de visada no comportamento espectral de imagens MODIS em áreas de Floresta Amazônica e Cerrado. *Geografia Ensino & Pesquisa*, v. 23, e10. <https://doi.org/10.5902/2236499434397>
- Santos, T.O.; Andrade Filho, V.S.; Rocha, V.M.; Menezes, J.S., 2017. Os impactos do desmatamento e queimadas de origem antrópica sobre o clima da Amazônia brasileira: um estudo de revisão. *Revista Geográfica Acadêmica*, v. 11, (2), 157-181.
- Santos, F.A.A.; Rocha, E.J.P.; Santos, J.S., 2019. Dinâmica da Paisagem e seus Impactos Ambientais na Amazônia. *Revista Brasileira de Geografia Física*, v. 12, (5), 1794-1815. <https://doi.org/10.26848/rbgf.v12.5.p1794-1815>
- Senay, G.B.; Bohms, S.; Singh, R.K.; Gowda, P.H.; Velpuri, N.M.; Alemu, H.; Verdin, J.P., 2013. Operational Evapotranspiration Mapping Using Remote Sensing and Weather Datasets: A New Parameterization for the SSEB Approach. *Journal of the American Water Resources Association*, v. 49, (3), 577-591. <https://doi.org/10.1111/jawr.12057>
- Serrão, E.A.O.; Lima, A.M.M.; Sousa, F.A.S.; Ferreira, T.R.; Santos, C.A.; Junior, J.A.S., 2017. Distribuição espacial de intensidade pluviométrica na calha do rio Solimões: estudo de caso da seca de 2010 na Amazônia. *ACTA Geográfica*, v. 11, (25), 1-16. <https://doi.org/10.18227/2177-4307.acta.v11i25.2904>
- Shapiro, S.S.; Wilk, M.B., 1965. An analysis of variance test for normality (complete samples). *Biometrika*, v. 52, (3/4), 591-611. <https://doi.org/10.2307/2333709>
- Silva, V.V.C.; Rezende, E.N., 2021. Os rios voadores e as mudanças climáticas ocasionadas pelo desmatamento da Floresta Amazônica: uma perspectiva a partir do constitucionalismo latino-americano. *Revista Brasileira de Direito Animal*, v. 16, (3), 96-113. <https://doi.org/10.9771/rbda.v16i3.47626>
- Silva, H.J.F.; Gonçalves, W.A.; Bezerra, B.G.; Silva, C.M.S.; Oliveira, C.P.; Mutti, P.R., 2022. Analysis of the influence of deforestation on the microphysical parameters of clouds in the Amazon. *Remote Sensing*, v. 14, (21), 1-23. <https://doi.org/10.3390/rs14215353>
- Souza, V.A.S.; Rotunno Filho, O.C.; Moreira, D.M.; Rudke, A.P.; Rocha Tortureli de Sá, M., 2019. Dinâmica do desmatamento na Amazônia e seus impactos na hidrologia: bacia do Rio Machadinho - Rondônia/Brasil. *Ciência Florestal*, v. 29, (3), 1004-1018. <https://doi.org/10.5902/1980509835333>
- Spera, S.A.; Galford, G.L.; Coe, M.T.; Macedo, M.N.; Mustard, J.F., 2016. Land-use change affects water recycling in Brazil's last agricultural frontier. *Global Change Biology*, v. 22, (10), 3405-3413. <https://doi.org/10.1111/gcb.13298>
- Stickler, C.M.; Coe, M.T.; Costa, M.H.; Soares-Filho, B.S., 2013. Dependence on hydroelectric power generation in the forests of the Amazon Basin at local and regional scales. *Proceedings of the National Academy of Sciences of the United States of America*, v. 110, (23), 9601-9606. <https://doi.org/10.1073/pnas.1215331110>
- Sun, L.; Baker, J. C. A.; Gloor, E.; Spracklen, D.; Boesch, H.; Somkuti, P.; Maeda, E.; Buermann, W., 2019. Seasonal and Inter-annual Variation of Evapotranspiration in Amazonia Based on Precipitation, River Discharge and Gravity Anomaly Data. *Frontiers in Earth Science*, v. 7, (32). <https://doi.org/10.3389/feart.2019.00032>
- Tomasella, J.; Marengo, J.A., 2011. A seca de 2010 na Amazônia. *Science*, v. 331, (6017), 532. <https://doi.org/10.1126/science.1200807>
- Trambauer, P.; Dutra, E.; Maskey, S.; Werner, M.; Pappenberger, F.; van Beek, L.P.H.; Uhlenbrook, S., 2014. Comparison of different evaporation estimates over the African continent. *Hydrology and Earth System Sciences*, v. 18, (1), 193-212. <https://doi.org/10.5194/hess-18-193-2014>
- Velásquez, C.; Queiroz, H.; Bernasconi, P., 2010. Fique por Dentro: a Bacia do Rio Xingu em Mato Grosso. ISA, São Paulo; Instituto Centro de Vida, Cuiabá.
- Vendruscolo, J.; Santos Júnior, N.R.F.; Macedo, T.M.; Donegá, M.V.B.; Fulan, J.Á.; Souza, R.F.S.; Cavalheiro, W.C.S., 2022. Características hidrogeomorfológicas e dinâmica da cobertura do solo na microbacia do rio Ariranha, Amazônia Ocidental. *Revista Científica Multidisciplinar*, v. 3, (1), e311034. <https://doi.org/10.47820/recima21.v3i1.1034>
- Warren, M.S., 2013. Desagregação espacial de estimativas de evapotranspiração real obtidas a partir do sensor MODIS. *Revista Brasileira de Meteorologia*, v. 28, (2), 153-162. <https://doi.org/10.1590/S0102-77862013000200004>
- Yang, X.; Ren, L.; Singh, V. P.; Liu, X.; Yuan, F.; Jiang, S.; Yong, B., 2012. Impacts of land use/land cover changes on evapotranspiration and runoff at Shalamulun River watershed, China. *Hydrology Research*, v. 43, (1-2), 23. <https://doi.org/10.2166/nh.2011.120>
- Zelazowski, P.; Malhi, Y.; Huntingford, C.; Sitch, S.; Fisher, J.B., 2011. Changes in the potential distributions of humid tropical forests on a warmer planet. *Philosophical Transactions of the Royal Society of London – Biological Sciences*, v. 369, (1934), 137-160. <https://doi.org/10.1098/rsta.2010.0238>
- Zhang, Y.; Kong, D.; Gan, R.; Chiew, F. H. S.; McVicar, T. R.; Zhang, Q.; Yang, Y., 2019. Coupled estimation of 500 m and 8-day resolution global evapotranspiration and gross primary production in 2002–2017. *Remote Sensing of Environment*, v. 222, (1), 165-182. <https://doi.org/10.1016/j.rse.2018.12.031>
- Zhang, X.; Wang, G.; Xue, B.; Wang, Y.; Wang, L., 2022. Spatiotemporal variation of evapotranspiration on different land use/cover in the inner Mongolia reach of the Yellow River Basin. *Remote Sensing*, v. 14, (18), 4499. <https://doi.org/10.3390/rs14184499>